Supplementary Figure 1

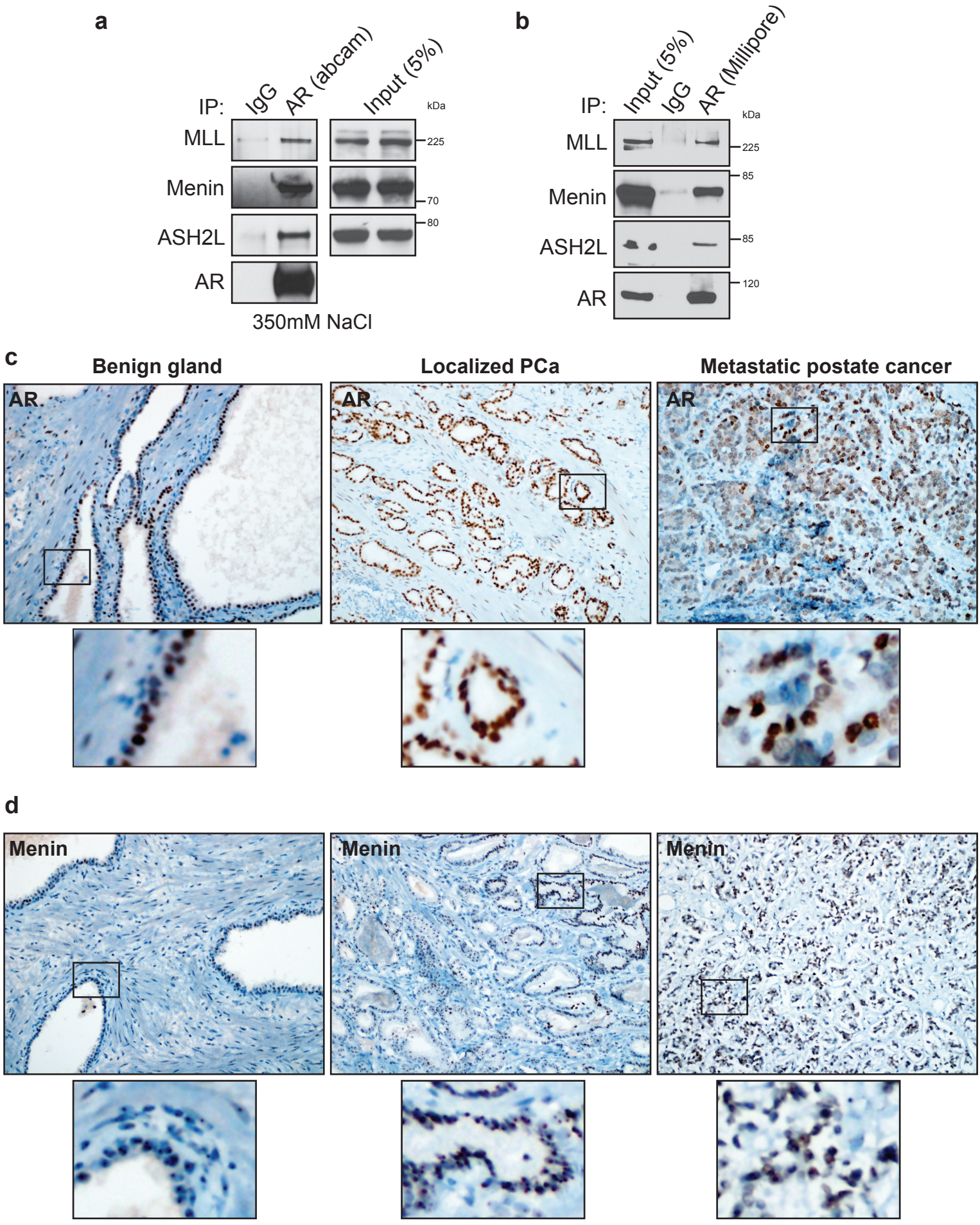

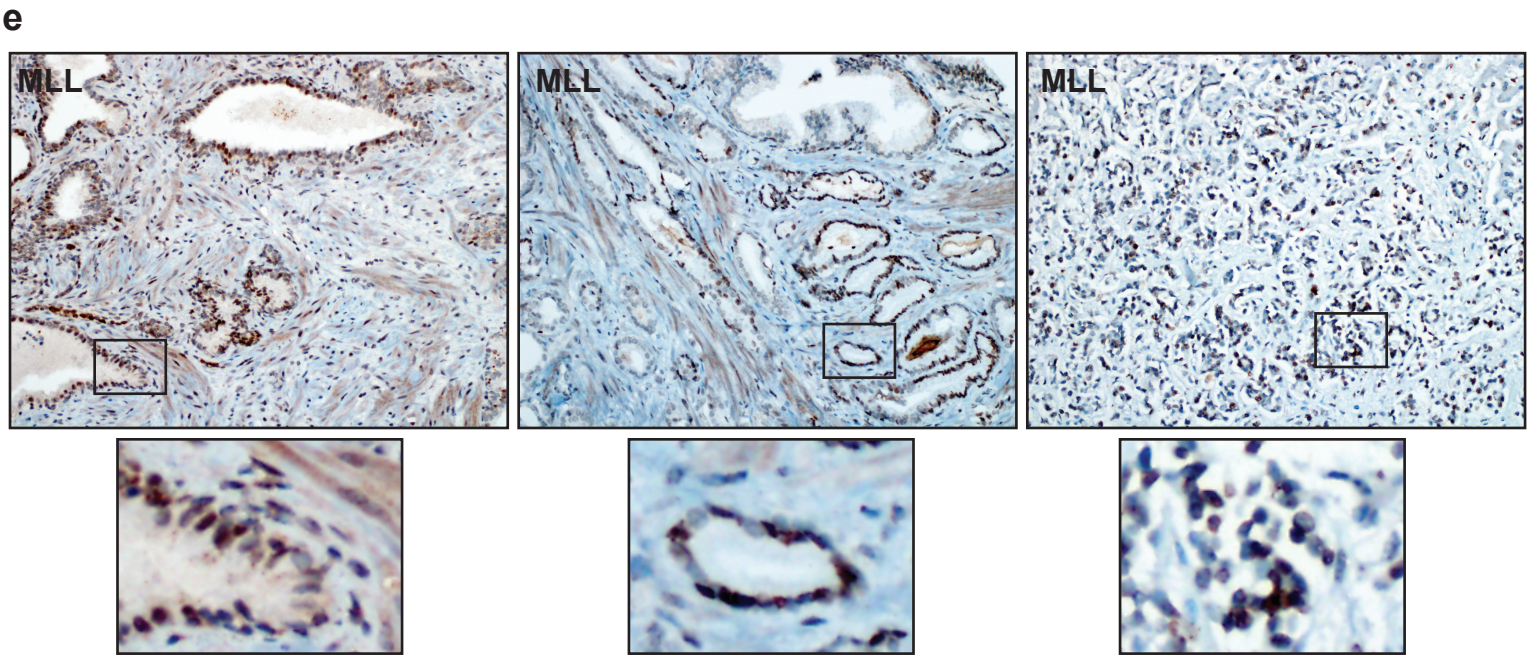

Supplementary Fig. 1: AR interacts with the MLL complex proteins. (**a**) VCaP nuclear lysates were subjected to immunoprecipitation (IP) in presence of 350mM Sodium Chloride (NaCl) followed by immunoblotting with indicated antibodies. (**b**) VCaP nuclear lysates were subjected to immunoprecipitation (IP) using anti-AR antibody (Millipore-06-680) followed by immunoblotting with indicated antibodies. Representative blots are shown (*n*=2). (**c-e**) Prostate tissue sections (benign, localized prostate cancer (PCa) and metastatic prostate cancer) stained with anti-AR (Santa Cruz, sc-816) (c), anti menin (Santa Cruz, sc-390345) (d) and anti-MLL (Santa Cruz, sc-18214) (e) antibodies. Insets show 40X magnifications.

Supplementary Figure 2

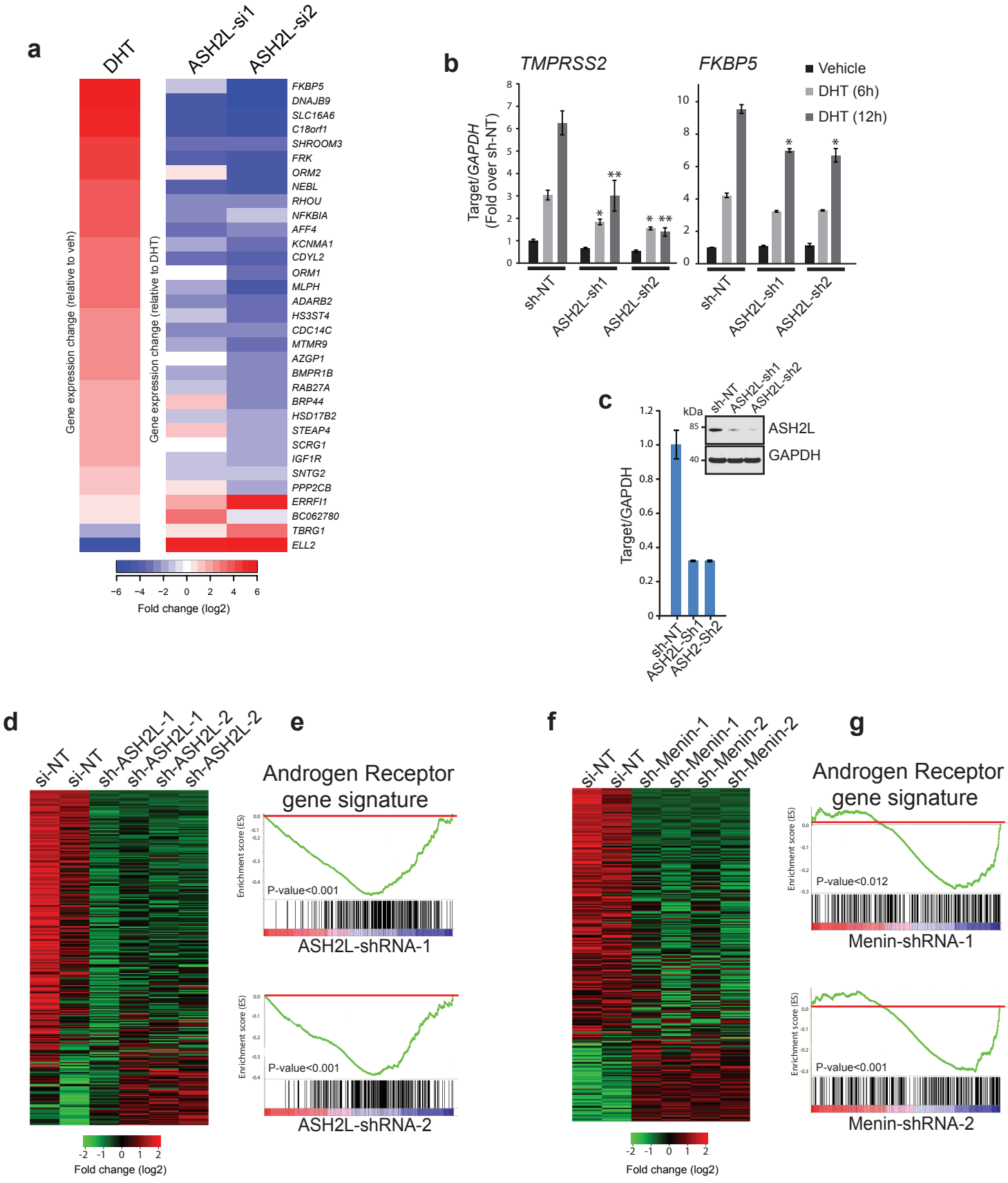

Supplementary Fig. 2: MLL complex proteins are important for AR signaling. (**a**) A heatmap representation of AR targets repressed by knockdown of ASH2L using two independent siRNA. (**b**) Expression of FKBP5 and TMPRSS2 as measured using quantitative polymerase chain reaction (qPCR, *n* = 3, mean ± s.e.m) in LNCaP cells stably expressing either non-targeting (NT) shRNA or two independent ASH2L shRNAs after 10nM DHT stimulation for 6 and 12 hours. (**c**) Efficiency of ASH2L knockdown was determined at transcript and protein levels using qPCR and immunoblotting respectively. (**d**) Heatmap represents the reversal of androgen-induced target gene expression profiles in LNCaP cells upon ASH2L knockdown using two independent shRNA. (**e**) GSEA using an AR target gene signature. (**f**) Heatmap represents the reversal of androgen-induced target gene expression profiles in LNCaP cells upon menin knockdown using two independent shRNA. (**g**) GSEA using AR target gene signature was performed.

Supplementary Figure 3

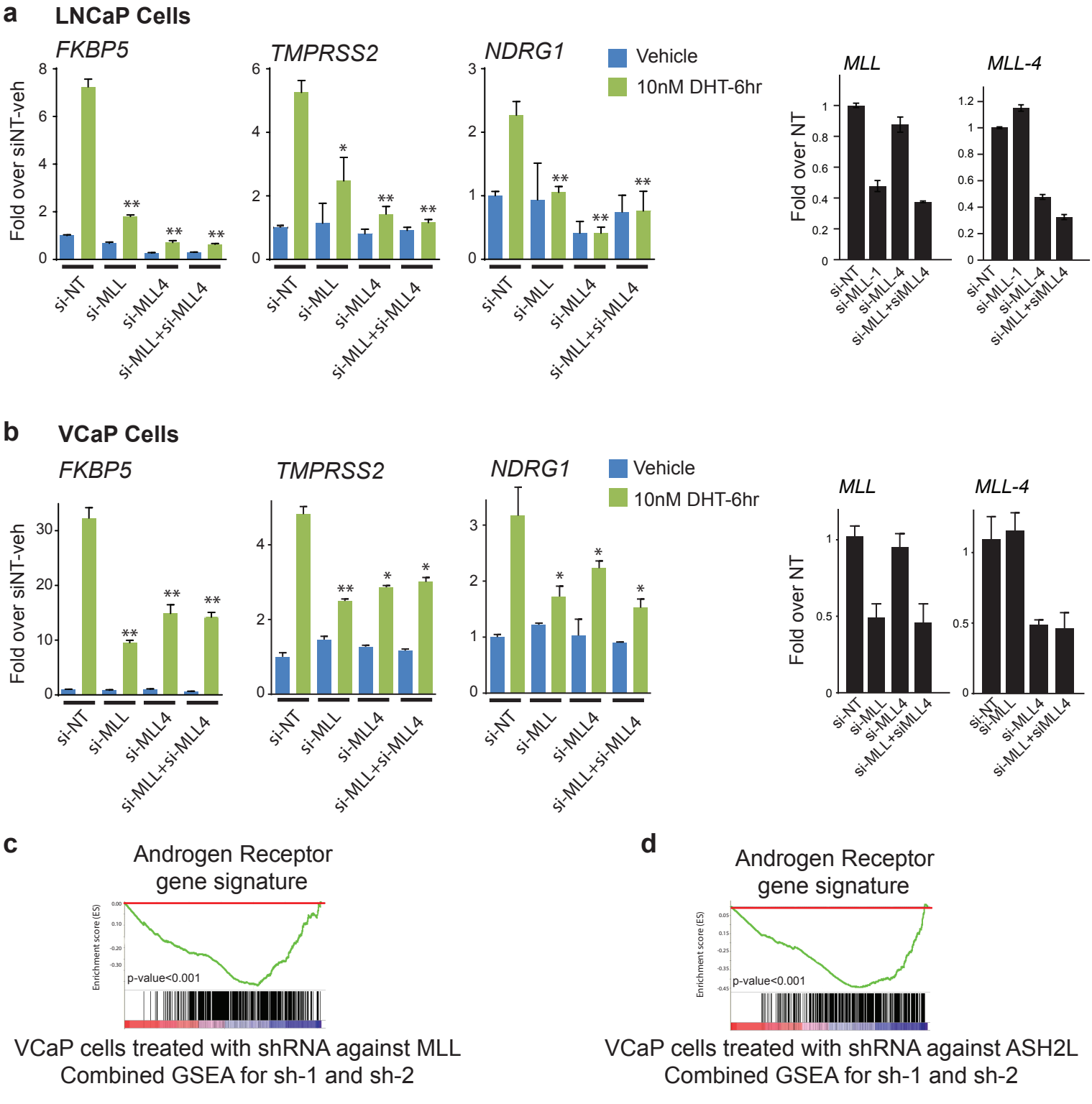

Supplementary Fig. 3: MLL and MLL4 are important for AR signaling. (**a,b**) LNCaP and VCaP cells were transfected with siRNA targeting *MLL, MLL4* or both (*MLL+MLL4*). Expression of AR target genes was quantified by qPCR after stimulation of cells with either 10nM DHT or vehicle for 6hours.. Knockdown efficiency was determined by qPCR for both *MLL* and *MLL4* transcripts. Bars represent mean ± s.e.m. (*n*=3). (**c,d**) GSEA against an AR target gene signature was performed on gene expression profiles obtained from VCaP cells stably expressing non-targeting (NT) shRNA or two independent MLL shRNA (c) or two independent ASH2L shRNA (d) post 10nM DHT stimulation. Average expression profiles from two independent shRNA treatments were used for GSEA analysis.

Supplementary Figure 4

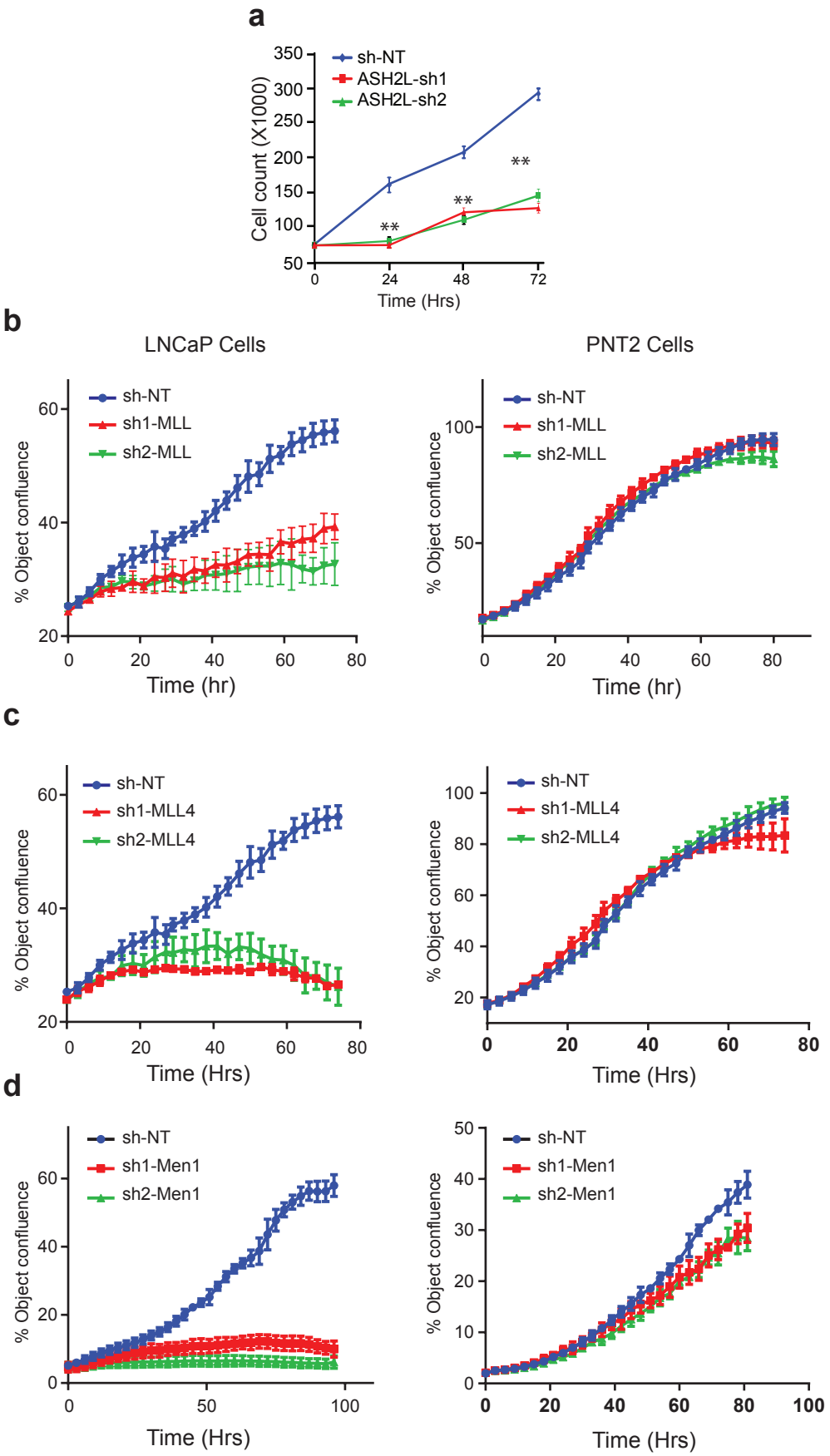

Supplementary Fig. 4: MLL complex proteins are important for cell proliferation. (**a**) Cell count for VCaP cells expressing NT shRNA or two independent *ASH2L* shRNAs respectively. (**b-d**) Cell proliferation was monitored using IncuCyte ZOOM live cell monitoring system in LNCaP and PNT2 cells transfected with NT shRNA or shRNA targeting *MLL* (b), *MLL4* (c) and *menin* (d). Error bar represents mean ± s.e.m (*n*=3).

Supplementary Figure 5

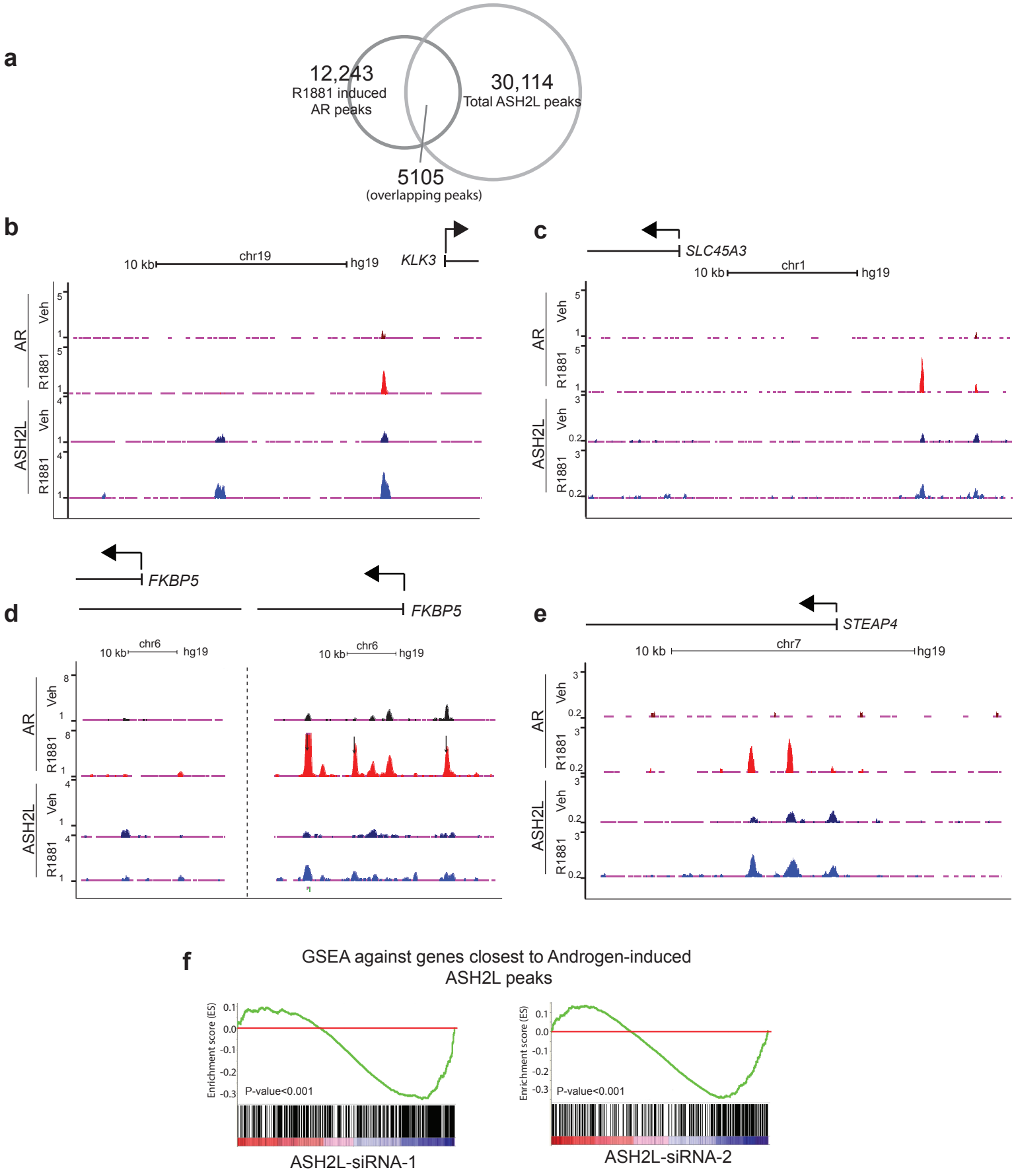

Supplementary Fig. 5: AR and ASH2L bind to the same genomic loci upon AR stimulation. (**a**) The overlap between androgen-induced AR peaks and total ASH2L peaks. (**b-e**) UCSC genome browser view of AR and ASH2L binding sites in *KLK3*(PSA) (b), *SLC45A3* (c), *FKBP5* (d) and *STEAP4* (e) gene promoters respectively. (**f**) GSEA was performed on ASH2L siRNA-1 and 2 gene expression microarray data (from Figure 2a) using a gene signature comprised of genes located within 10kb of androgen-induced ASH2L peaks (Supplementary Table 2).

Supplementary Figure 6

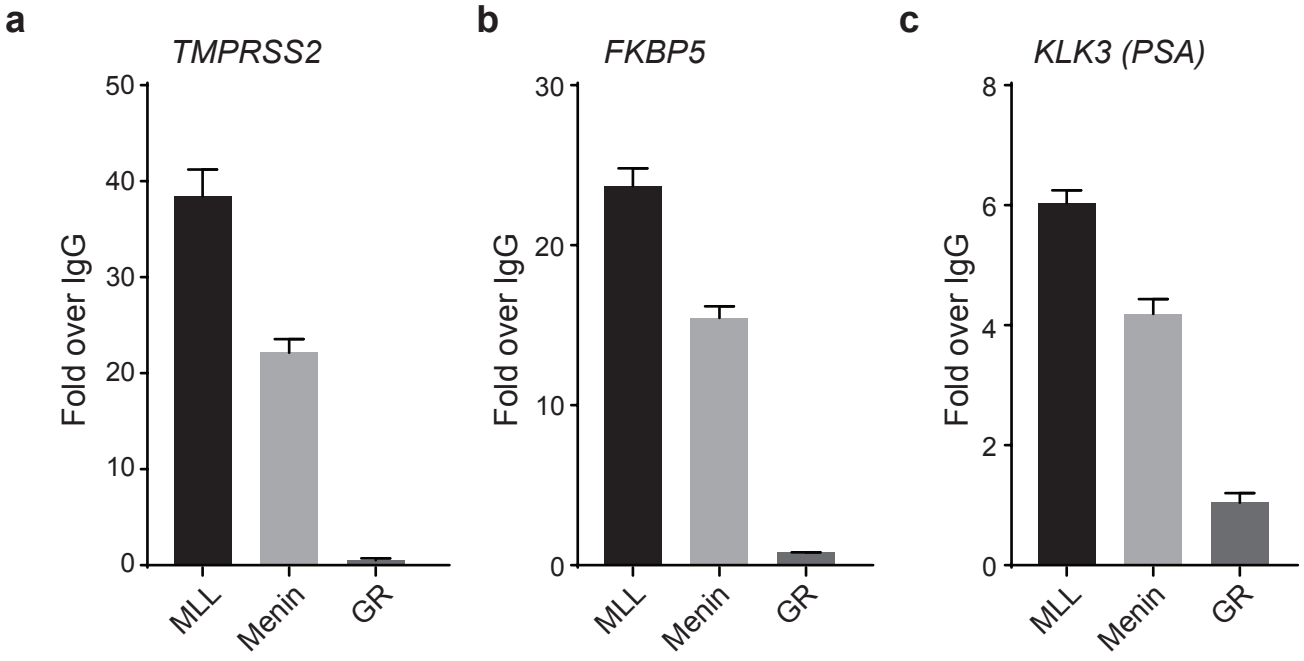

Supplementary Fig. 6: Menin and MLL binds to AR target genes. (**a-c**) ChIP-PCR to assess the enrichment of MLL, menin and glucocorticoid receptor (GR) binding on AR targets gene promoters including *TMPRSS2*, *FKBP5* and *KLK3* (PSA). Bars represent mean ± s.e.m (*n*=3).

Supplementary Figure 7

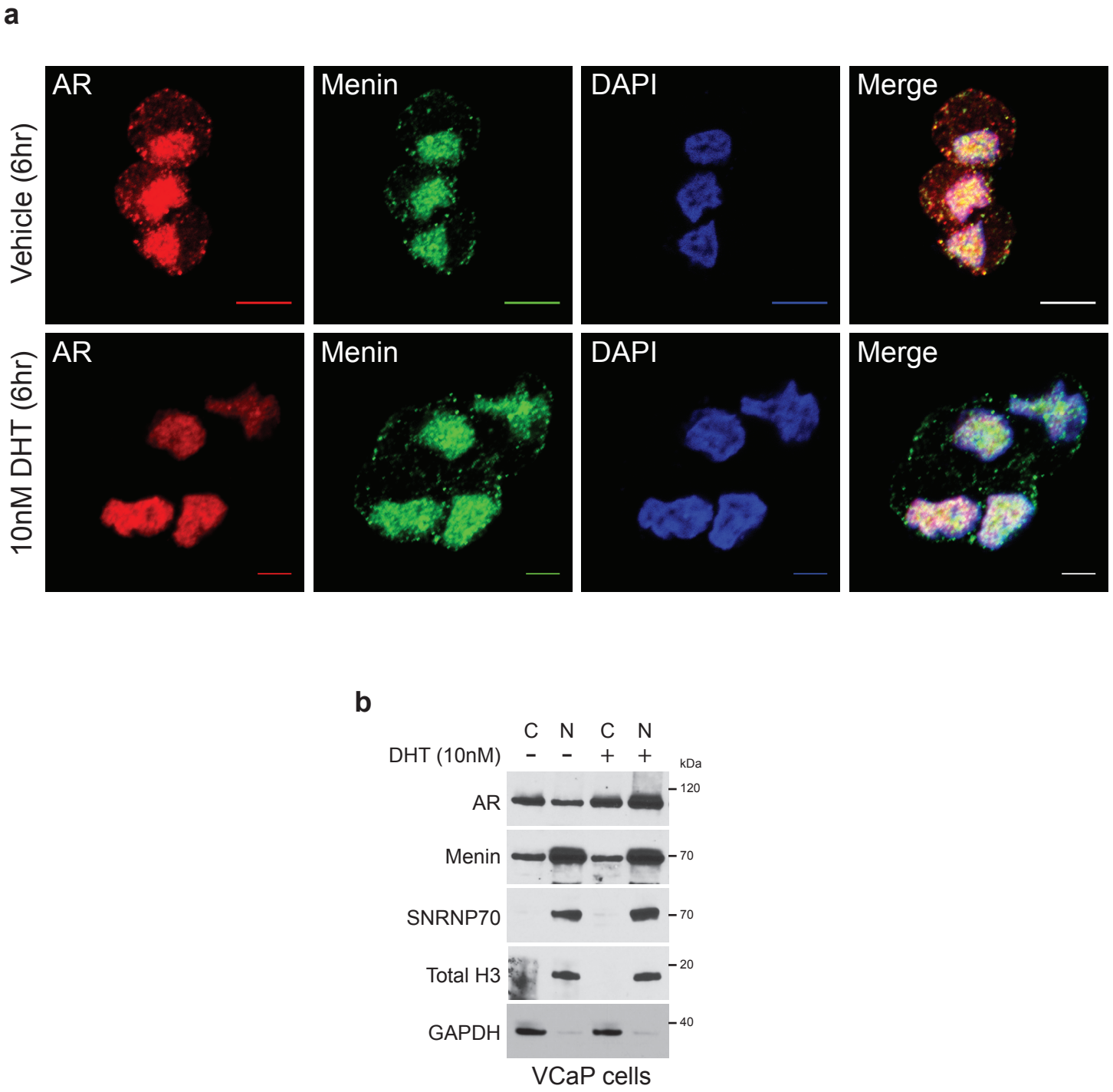

Supplementary Fig. 7: Distribution of Menin upon AR stimulation**.** (**a**) AR (red) and Menin (green) protein localization was monitored by immunofluorescence in VCaP cells 6 hours after treatment with either vehicle (top panel) or 10nM DHT (bottom panel). Shown are representative micrographs from two independent experiment (**b**) Cellular distribution of various proteins was analyzed by western blotting in VCaP cytoplasmic and nuclear extracts from either vehicle or 10nM DHT treated cells. Shown are representative blots (*n*=2).

Supplementary Figure 8

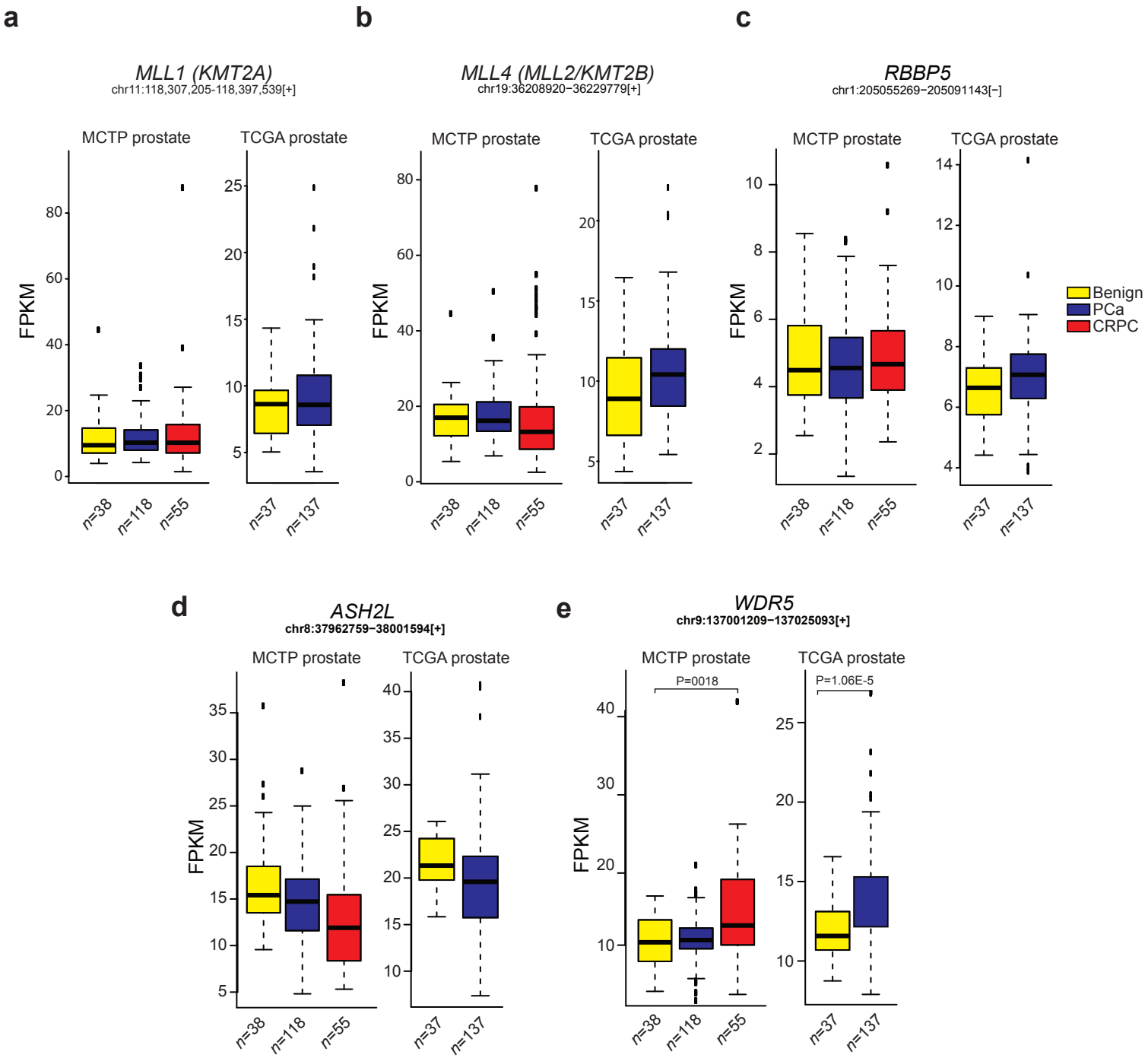

Supplementary Fig. 8: Expression of MLL complex proteins. (**a-e**) Expression of *MLL, MLL4, ASH2L, RBBP5* and *WDR5* in RNA-Seq data from 38 benign, 118 localized prostate cancer (PCa) and 55 castrate resistant prostate cancer (CRPC) tissues in MCTP cohort and in RNA-Seq data from 37 benign prostate and 137 PCa from the TCGA cohort. The y-axis denotes Fragments Per Kilobase of transcript per Million mapped reads (FPKM).

Supplementary Figure 9

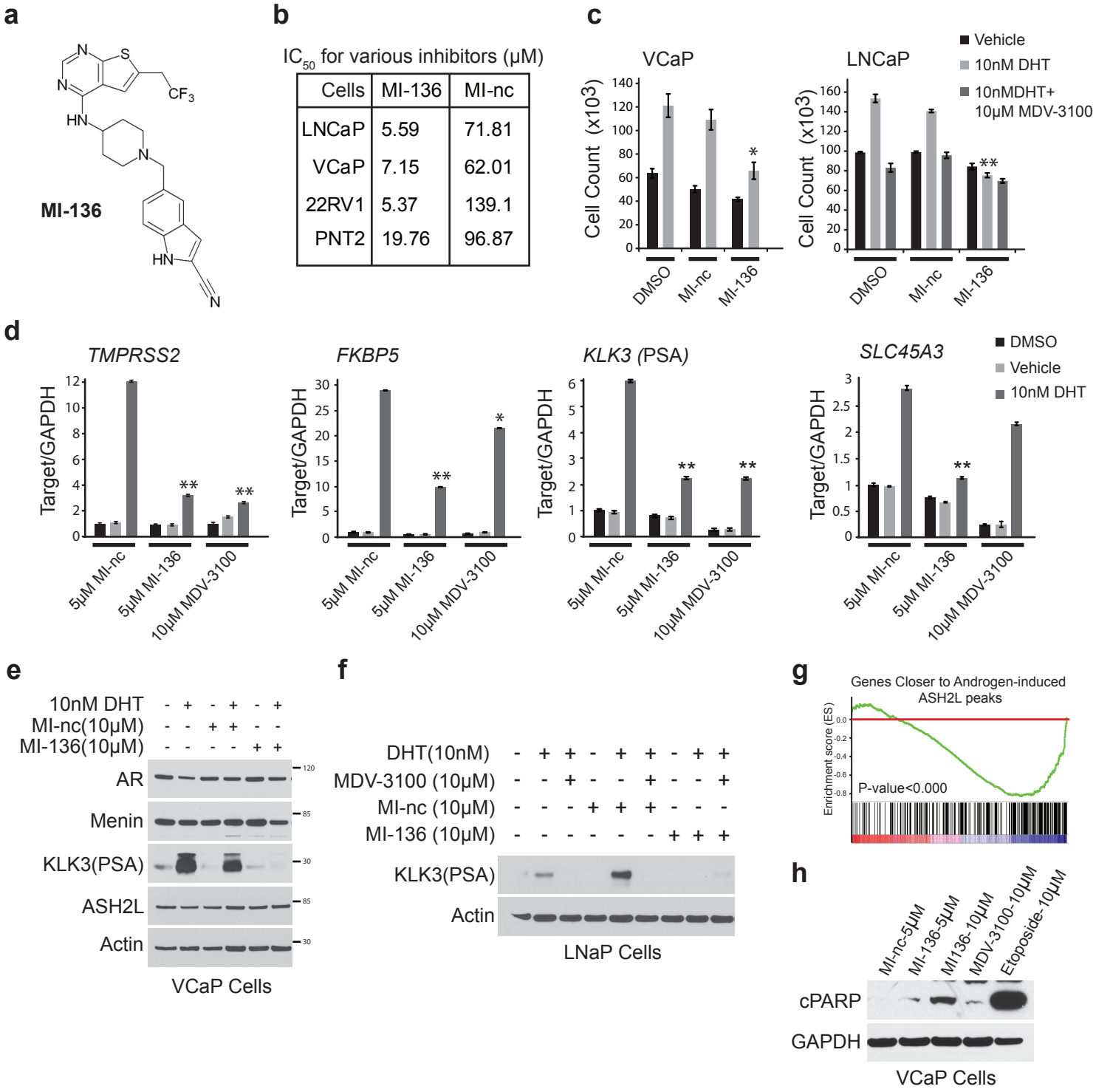

Supplementary Fig. 9: *In vitro* effects of MI-136. (**a**) Chemical structure of menin-MLL inhibitor MI-136. (**b**) IC_{50} values of MI-136 and MI-nc (control) in various cell lines. (**c**) VCaP and LNCaP cells were treated with DMSO, 5μM MI-136 or 5μM MI-nc, and the effect on growth was measured by cell counting after 5 days of DHT stimulation in the presence or absence of MDV-3100. Bars represent mean ± s.e.m (*n*=4). (**d**) VCaP cells were pre-treated with various inhibitors and stimulated with 10nM DHT for 12 hours. The effect on gene expression was quantified by qPCR. Bars represent mean ± s.e.m (*n*=3) (**e**) VCaP cells were pre-treated with the indicated inhibitors and stimulated with 10nM DHT for 24 hours. The effects on protein levels were determined by immunoblotting using indicated antibodies. (**f**) LNCaP cells were pre-treated with the indicated inhibitors and stimulated with 10nM DHT for 24 hours. The effects on protein levels were determined by immunoblotting using indicated antibodies. (**g**) GSEA was performed using a signature comprised of genes that were within 10kb of androgen-induced ASH2L ChIP-Seq peaks.(**h**)VCaP cells were treated with indicated inhibitors. Effect on apoptosis was estimated by immunoblotting using antibody that specifically recognizes cleaved PARP. All the blots shown in the figure are representative of three independent experiments.

Supplementary Figure 10

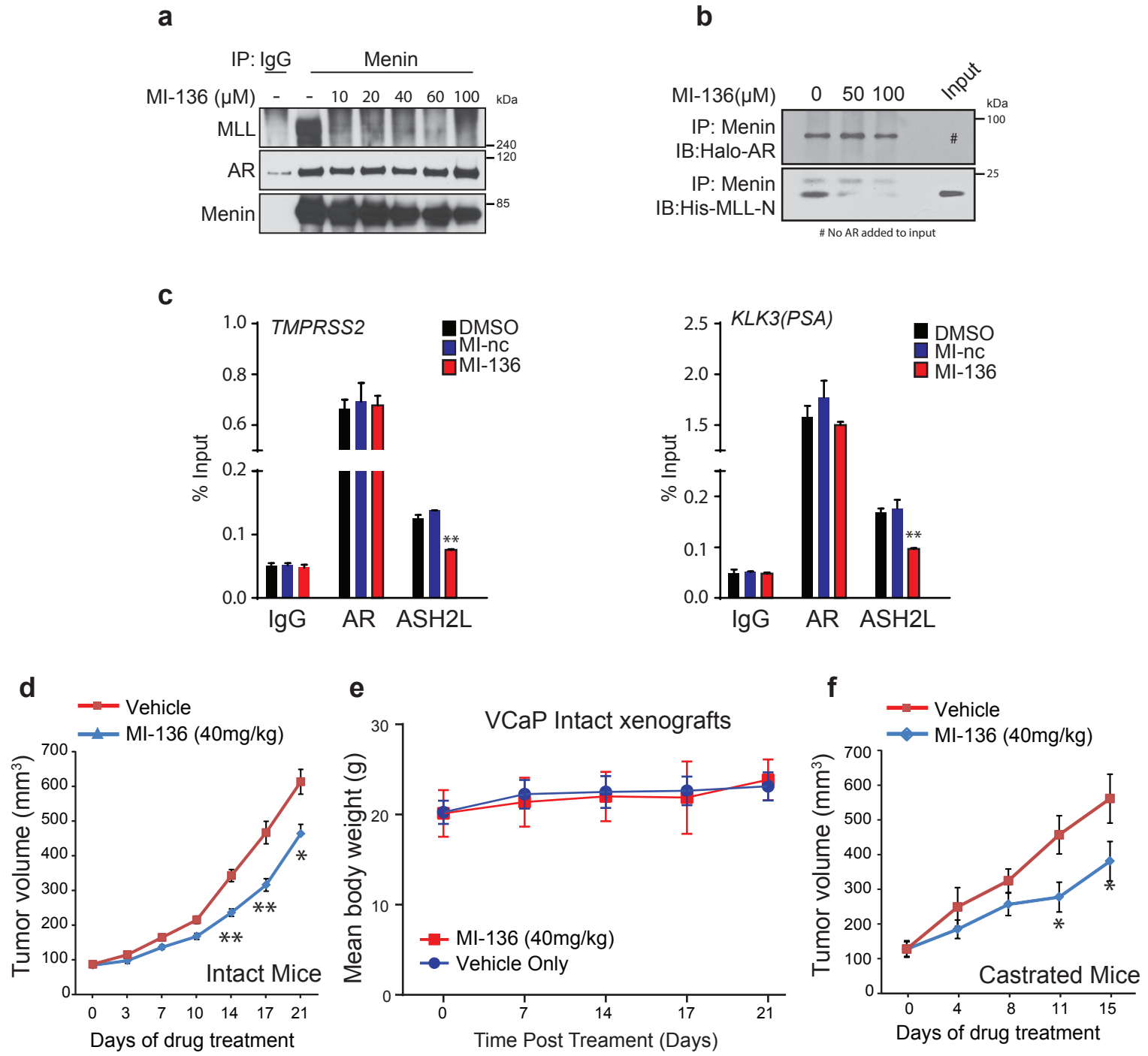

Supplementary Fig. 10: Effect of MI-136 on growth of VCaP xenografts. (**a**) Menin IP-Western in VCaP cells subjected to 48 hour treatment with varying concentration of MI-136 to assess MLL and AR proteins. (**b**) *In vitro* Menin IP-western with purified menin, halo-tagged full-length (FL) AR and His-tagged MLL-N-terminal region proteins in presence of increasing MI-136 concentrations. Menin immunoprecipitates were subjected to western analysis using anti-His and anti-AR antibodies. Shown are representative blots from two independent experiments. (**c**) ChIP-PCR for AR and ASH2L binding to *TMPRSS2* and *KLK3* (PSA) promoters. Quantitative real-time ChIP PCRs were performed in VCaP cells were treated with 10μM MI-136 or MI-nc for 24 hours. Bars represent mean ± SEM (n=3) from one of two independent experiments. *, P<0.05; comparision with DMSO by one-way ANOVA. (**d**) Once the tumors reach 80-100mm^3, mice were treated intra-peritoneal with either vehicle (n=16) or 40mg/kg MI-136 (n=16) and tumor caliper measurements were taken bi-weekly. (**e**) Mean body weight of mice over time after treatment with MI-136. (**f**) Effect of MI-136 on growth of castrate-resistant VCaP xenografts. Tumors were grown as outlined in Supplementary Fig. 12c. Once the tumors had regressed to 80-100 mm^3 following castration, mice received intra-peritoneal injections of either vehicle (n=12) or 40mg/kg MI-136 (n=12) 5 days/week. Tumor caliper measurements were recorded bi-weekly. *, P<0.05; **, P<0.005. Compared with Vehicle by t-test. Error bars represent ± s.e.m.

Supplementary Figure 11

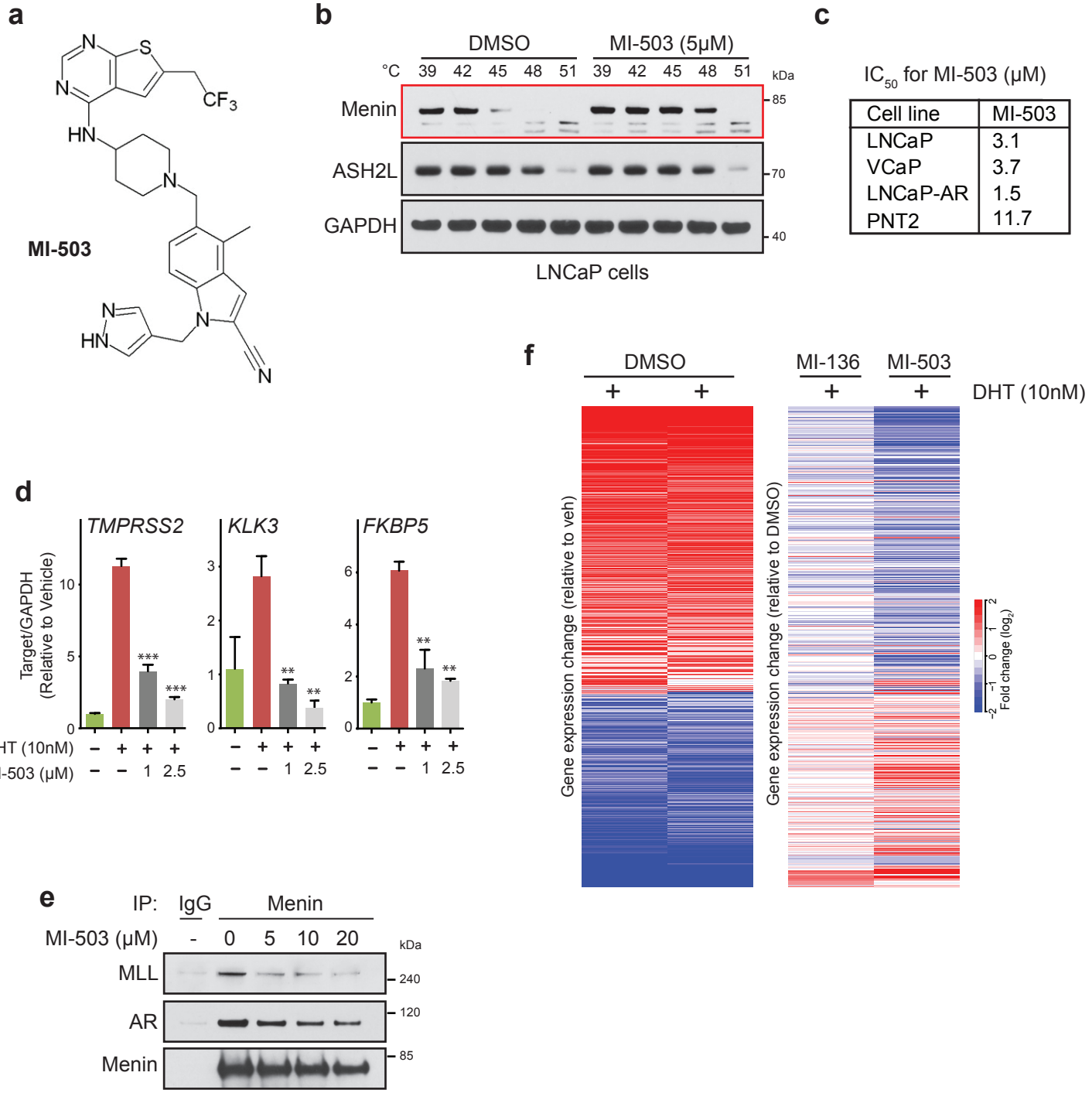

Supplementary Fig. 11: *In vitro* effects of MI-503. (**a**) Chemical Structure of menin-MLL inhibitor MI-503. (**b**) LNCaP cells were treated with 5μM MI-503 and incubated at indicated temperatures. Cells were lysed and soluble proteins were detected by immunoblotting. (**c**) IC_{50} values of MI-503 in various prostate cell lines. (**d**) The effect on AR target gene expression (*TMPRSS2, FKBP5,* and *KLK3*) was quantified by qPCR in LNCaP cells pre-treated with either DMSO or MI-503 and subsequently stimulated with 10nM DHT for 6 hours (*n* = 3, mean ± s.e.m). (**e**) VCaP cells were treated with varying concentration of MI-503 for 48 hrs followed by immunoprecipitation of menin. Immunoprecipitates were assessed for MLL and AR by immunoblotting. Shown are representative blots (*n*=2). (**f**) A Heatmap comparing the effect of MI-136 (5μM) and MI-503 (5μM) on DHT promoted gene expression in VCaP cells.

Supplementary Figure 12

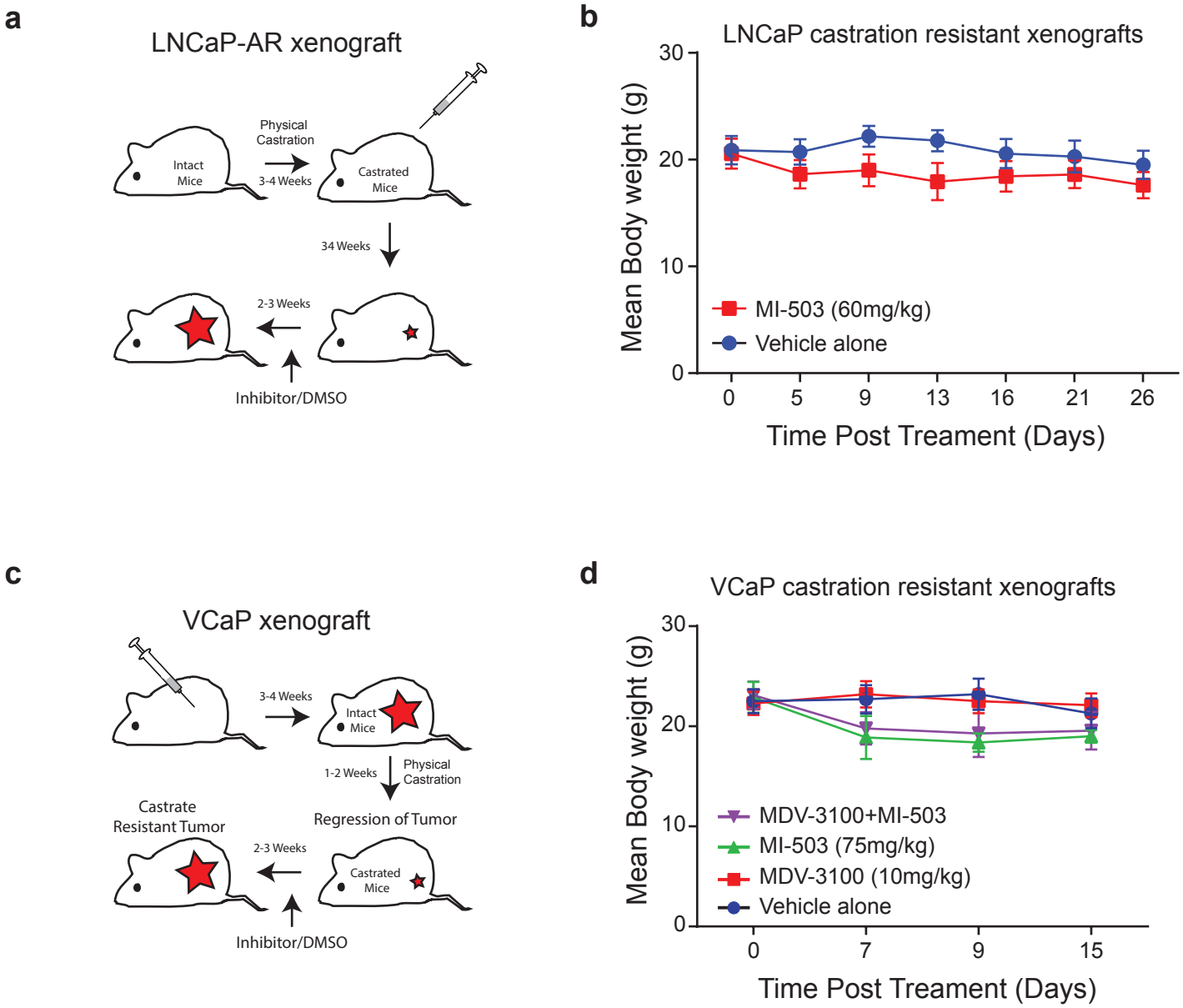

Supplementary Fig. 12: Effect of MI-503 on *in vivo* tumor growth. (**a**) A schematic representation of experimental workflow to evaluate the effect of MI-503 on LNCaP-AR xenograft growth in castrated mice. (**b**) Mean (± s.e.m.) body weight of mice over time after treatment with vehicle or MI-503. (**c**) A schematic representation of experimental workflow to evaluate the effect of MI-136 and MI-503 on growth of castrate-resistant VCaP xenograft. (**d**) Mean body (± s.e.m.) weight of mice over time after treatment with vehicle, MI-503, MDV-3100 or combination (MI-503+MDV-3100).

Supplementary Figure 13

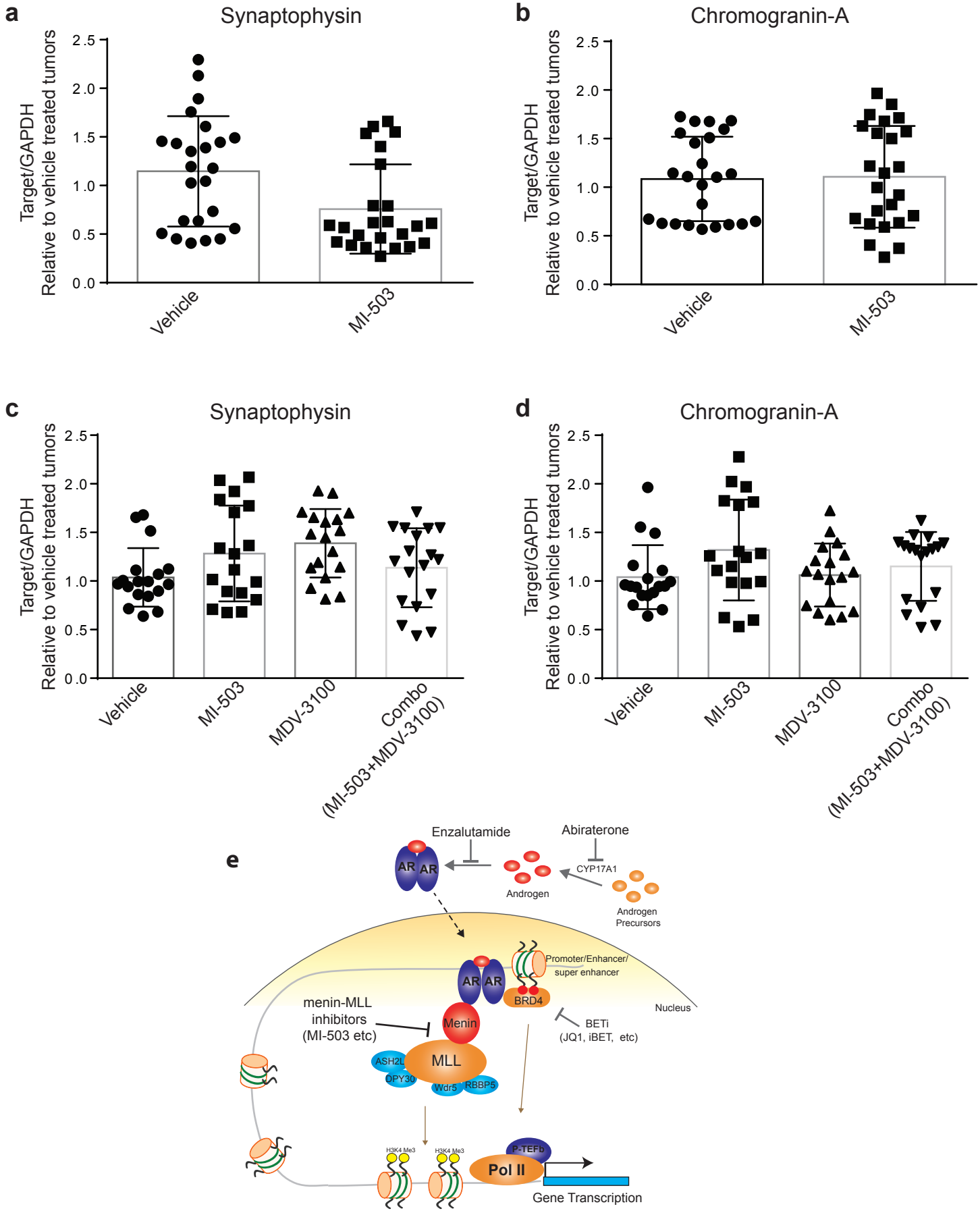

Supplementary Figure 13: Effect of MI-503 on expression of neuroendocrine differentiation markers**.** (**a-d**) Total RNA was isolated from LNCaP-AR (a,b) and VCaP (c,d) xenografts after treatment with specific inhibitors. Expression of neuroendocrine makers including Synaptophysin and Chromogranin-A was measured by qRT-PCR. Each dot represents individual tumor samples. All data throughout the figure are shown as the mean ± s.e.m (**e**) A proposed model for the role of the MLL complex in the AR transcriptional program.